16th World Congress in Computational Mechanics (WCCM)
21-26 July 2024, Vancouver, Canada
A. Korobenko, M. Laforest, S. Prudhomme, R. Vaziri (Eds)

DETERMINATION OF HIGH-ORDER FREQUENCY RESPONSE OF NONLINEAR SYSTEMS USING THE ARC-LENGTH METHOD

LUCAS P. TANABE[1] **AND ALBERTO L. SERPA**[2]

[1] Department of Computational Mechanics, School of Mechanical Engineering, UNICAMP
R. Mendeleyev, 200 - Cidade Universitária, Campinas - SP, Brazil
l147046@dac.unicamp.br

[2] Department of Computational Mechanics, School of Mechanical Engineering, UNICAMP
R. Mendeleyev, 200 - Cidade Universitária, Campinas - SP, Brazil
alserpa@unicamp.br

Key words: Nonlinear, Frequency response, Harmonic balance, Arc-length, Oscillator.

Abstract. While linear systems have been extensively studied in the past few decades, systems with strong nonlinearities are not as widely investigated. One of the reasons why these are less applied in engineering is due to the fact that solving nonlinear equations usually demands a steep increase in processing capacity and time when compared to their linear counterparts. As computers become more powerful, significantly more advanced nonlinear systems can be studied and analyzed, providing solutions that are more accurate for real-world applications.

When it comes to frequency analysis, it is possible that nonlinear frequency response shows the phenomena of hardening or softening. In this case, the resonance peaks of the frequency response are tilted to the right or left, respectively, in comparison with linear frequency response. The consequences of these phenomena might prove essential to safety assessment of real-life structures as the resonance peak might greatly differ from those obtained in a linear analysis.

In this study, the high-order frequency response of the Helmholtz-Duffing oscillator is analyzed in order to evaluate its influence on the system. The oscillator exhibits Duffing nonlinearities represented by cubic springs and Helmholtz nonlinearities represented by quadratic springs. The high-order harmonic balance method was used to determine the dynamic equation in the frequency domain. The nonlinearities were numerically integrated based on the coefficients of the Fourier series. Originally used to find the solution path of nonlinear static structural analyses, the arc-length method was adapted to determine the nonlinear frequency response.

The equations from the first-order harmonic balance method assume that the nonlinear system response, as well as the nonlinear forces, are dominated by the fundamental harmonic. In this case, high-order harmonics are neglected. When it comes to high-order frequency response, multiple harmonics are considered in the system response and the equations are derived from the high-order harmonic balance method. This study shows that the behavior of systems with cubic stiffness only is usually very accurate with the first-order analysis. However, when quadratic stiffness is present, multiple harmonics must be taken into consideration in order to accurately

describe the system behavior. Otherwise, the frequency response is possibly inaccurate and sometimes chaotic as it is not entirely dominated by its fundamental harmonic.

1 INTRODUCTION

When it comes to mechanical structures, it is often assumed that nonlinear effects are either negligible or can be linearized to assess the behavior of certain mechanical systems. However, as the demand for lightweight design grows to achieve slender and thin structures, this approximation may no longer correctly predict the behavior of highly nonlinear structures.

In this study, the steady-state response of several classical nonlinear oscillators is analyzed. While systems such as the Duffing oscillator with cubic stiffness can be accurately represented by its fundamental harmonic, the presence of quadratic stiffness, as seen in the Helmholtz and Duffing-Helmholtz oscillators, renders first-order analysis inadequate. This issue can be addressed by introducing high-order harmonics into the system of equations.

The arc-length method, a continuation algorithm created to overcome critical points and instability zones of nonlinear static structural problems, was initially proposed by Riks [1] and later improved by Crisfield [2]. The method was then adapted to determine nonlinear frequency response curves of nonlinear systems [3].

In order to determine the system of equations in the frequency domain, the harmonic balance method was applied. This method has been widely used in a number of fields, from elctrical circuits with nonlinear elements [4] to computational fluid dynamics (CFD) models of unsteady flows [5] or nonlinear beams [6]. An alternative to this method is the describing functions method, as demonstrated in [7].

The high-order frequency response of the Duffing oscillator was explored in [8]. Other studies investigated the high-order response of systems such as the Van der Pol oscillator [9] and the unilateral spring oscillator [10]. The time response analysis of the Duffing-Helmholtz oscillator was examined in [11].

In this study, when high-order harmonics were considered in systems with quadratic nonlinearity, not only is the fundamental harmonic greatly affected, but high-order harmonics may present significant contributions to the overall system response at certain frequencies. The Duffing oscillator, with cubic stiffness only, exhibited satisfactory results when only the fundamental harmonic was considered.

2 THE HARMONIC BALANCE METHOD

The harmonic balance is a method used to compute the steady-state response of nonlinear systems, commonly applied to nonlinear electrical circuits or, as in this case, nonlinear mechanical oscillators. Essentially, it relies on the fact that a periodic solution to the system of nonlinear differential equations can be represented by a Fourier series, which is a combination of sinusoids at different frequencies.

The matrix equation of motion of a structure with internal nonlinearities $\boldsymbol{f}_{nl}$ subject to an external force vector $\boldsymbol{f}_e$ can be written as follows:

$$\boldsymbol{M}\ddot{\boldsymbol{x}} + \boldsymbol{C}\dot{\boldsymbol{x}} + \boldsymbol{K}\boldsymbol{x} + \boldsymbol{f}_{nl} = \boldsymbol{f}_e = \frac{\boldsymbol{F}}{2}e^{i\omega t} + \frac{\boldsymbol{F}^*}{2}e^{-i\omega t}, \tag{1}$$

where $\boldsymbol{x}$ is the displacement vector, $\boldsymbol{M}$ is the mass matrix, $\boldsymbol{C}$ is the damping matrix and $\boldsymbol{K}$ is the stiffness matrix. In this paper, only harmonic external forces are considered. Their excitation frequency is ω and $\boldsymbol{F}$ represents the complex excitation amplitude vector (and $\boldsymbol{F}^*$ its complex conjugate).

The steady-state solution can be written as a Fourier series [12] as shown in Equation (2). The s-th harmonic of the complex displacement amplitude vector is represented by $\boldsymbol{X}^{[s]}$.

$$\boldsymbol{x} = \sum_{s=-\infty}^{\infty} \frac{\boldsymbol{X}^{[s]}}{2} e^{is\omega t}, \tag{2}$$

where $\boldsymbol{X}^{[-s]}$ is the complex conjugate of $\boldsymbol{X}^{[s]}$.

2.1 First-Order Harmonic Balance

The First-Order Harmonic Balance method is used when the nonlinear forces and the system response are dominated by their fundamental harmonic. In this case, only the first term of the Fourier series is considered for the nonlinear force and for the response:

$$\boldsymbol{f}_{nl} = \frac{\boldsymbol{F}_{nl}^{[1]}}{2}e^{i\omega t} + \frac{\boldsymbol{F}_{nl}^{[-1]}}{2}e^{-i\omega t}, \tag{3}$$

$$\boldsymbol{x} = \frac{\boldsymbol{X}^{[1]}}{2}e^{i\omega t} + \frac{\boldsymbol{X}^{[-1]}}{2}e^{-i\omega t}. \tag{4}$$

Substituting Equations (3) and (4) into Equation (1) and isolating the terms that are followed by $e^{i\omega t}$, the system equation in the frequency domain is obtained:

$$(-\omega^2\boldsymbol{M} + i\omega\boldsymbol{C} + \boldsymbol{K})\boldsymbol{X}^{[1]} = \boldsymbol{F} - \boldsymbol{F}_{nl}^{[1]}(\boldsymbol{X}^{[1]}). \tag{5}$$

It is possible to rewrite Equation (5) by defining the complex dynamic stiffness matrix of the linear terms $\boldsymbol{Z}(\omega) = -\omega^2\boldsymbol{M} + i\omega\boldsymbol{C} + \boldsymbol{K}$:

$$\boldsymbol{Z}(\omega)\boldsymbol{X}^{[1]} = \boldsymbol{F} - \boldsymbol{F}_{nl}^{[1]}(\boldsymbol{X}^{[1]}). \tag{6}$$

2.2 High-Order Harmonic Balance

The High-Order Harmonic Balance method is used when the nonlinear forces and the system response may not be dominated only by their fundamental harmonic. In this case, other harmonics must be considered in order to accurately describe the system behaviour. The displacement vector and its derivatives are shown in Equations (7)-(9) considering the first h harmonics of the Fourier series, along with the static displacement, $\boldsymbol{x}_0 = \frac{\boldsymbol{X}_0}{2}$, which denotes the value around which the system oscillates.

$$\boldsymbol{x} = \sum_{s=-h}^{h} \frac{\boldsymbol{X}^{[s]}}{2} e^{is\omega t}, \tag{7}$$

$$\dot{\boldsymbol{x}} = \sum_{s=-h}^{h} is\omega \frac{\boldsymbol{X}^{[s]}}{2} e^{is\omega t}, \tag{8}$$

$$\ddot{\boldsymbol{x}} = \sum_{s=-h}^{h} -s^2\omega^2 \frac{\boldsymbol{X}^{[s]}}{2} e^{is\omega t}. \tag{9}$$

Similarly, the nonlinear forces can be approximated by the first h harmonics of the Fourier series:

$$\boldsymbol{f}_{nl} = \sum_{s=-h}^{h} \frac{\boldsymbol{F}_{nl}^{[s]}}{2} e^{is\omega t}. \tag{10}$$

The complex nonlinear force amplitude vector is given by the Fourier coefficients:

$$\boldsymbol{F}_{nl}^{[s]} = \frac{\omega}{\pi} \int_0^{\frac{2\pi}{\omega}} \boldsymbol{f}_{nl} \cos(s\omega t)\, dt - i\frac{\omega}{\pi} \int_0^{\frac{2\pi}{\omega}} \boldsymbol{f}_{nl} \sin(s\omega t)\, dt. \tag{11}$$

Substituting Equations (7)-(10) into Equation (1) and isolating the terms that are followed by $e^{is\omega t}$, the system equation for the $s\text{-}th$ harmonic is obtained ($s \neq 1$):

$$(-s^2\omega^2\boldsymbol{M} + is\omega\boldsymbol{C} + \boldsymbol{K})\boldsymbol{X}^{[s]} = -\boldsymbol{F}_{nl}^{[s]}(\boldsymbol{X}^{[0]}, \boldsymbol{X}^{[1]}, \boldsymbol{X}^{[2]}, ..., \boldsymbol{X}^{[h]}). \tag{12}$$

Rewriting Equation (12) with the complex dynamic stiffness matrix of the vibrating system:

$$\boldsymbol{Z}(s\omega)\boldsymbol{X}^{[s]} = -\boldsymbol{F}_{nl}^{[s]}(\boldsymbol{X}^{[0]}, \boldsymbol{X}^{[1]}, \boldsymbol{X}^{[2]}, ..., \boldsymbol{X}^{[h]}). \tag{13}$$

Adapting Equation (6) to take into consideration all harmonics $(\boldsymbol{X}^{[0]}, \boldsymbol{X}^{[1]}, \boldsymbol{X}^{[2]}, ..., \boldsymbol{X}^{[h]})$ and combining with Equation (13), it is possible to represent the system equation in the frequency domain for all harmonics:

$$\begin{bmatrix} \boldsymbol{K} & \mathbf{0} & \mathbf{0} & \dots & \mathbf{0} \\ \mathbf{0} & \boldsymbol{Z}(\omega) & \mathbf{0} & \dots & \mathbf{0} \\ \mathbf{0} & \mathbf{0} & \boldsymbol{Z}(2\omega) & \dots & \mathbf{0} \\ \vdots & \vdots & \vdots & \ddots & \vdots \\ \mathbf{0} & \mathbf{0} & \mathbf{0} & \dots & \boldsymbol{Z}(h\omega) \end{bmatrix} \begin{Bmatrix} \boldsymbol{X}^{[0]} \\ \boldsymbol{X}^{[1]} \\ \boldsymbol{X}^{[2]} \\ \vdots \\ \boldsymbol{X}^{[h]} \end{Bmatrix} = \begin{Bmatrix} \mathbf{0} \\ \boldsymbol{F} \\ \mathbf{0} \\ \vdots \\ \mathbf{0} \end{Bmatrix} - \begin{Bmatrix} \boldsymbol{F}_{nl}^{[0]}(\boldsymbol{X}^{[0]}, \boldsymbol{X}^{[1]}, \boldsymbol{X}^{[2]}, ..., \boldsymbol{X}^{[h]}) \\ \boldsymbol{F}_{nl}^{[1]}(\boldsymbol{X}^{[0]}, \boldsymbol{X}^{[1]}, \boldsymbol{X}^{[2]}, ..., \boldsymbol{X}^{[h]}) \\ \boldsymbol{F}_{nl}^{[2]}(\boldsymbol{X}^{[0]}, \boldsymbol{X}^{[1]}, \boldsymbol{X}^{[2]}, ..., \boldsymbol{X}^{[h]}) \\ \vdots \\ \boldsymbol{F}_{nl}^{[h]}(\boldsymbol{X}^{[0]}, \boldsymbol{X}^{[1]}, \boldsymbol{X}^{[2]}, ..., \boldsymbol{X}^{[h]}) \end{Bmatrix}. \tag{14}$$

3 NONLINEAR FREQUENCY RESPONSE CURVES

The frequency response curves of some nonlinear systems exhibit a phenomenon where the resonance peak becomes inclined. When the resonance peak tilts to the right, this phenomenon is called hardening, while if it tilts to the left, the phenomenon is called softening. Figure 1 shows a comparison of two frequency response curves. The first curve is from a single-degree-of-freedom (SDOF) linear system, while the other is from an SDOF nonlinear system with cubic stiffness.

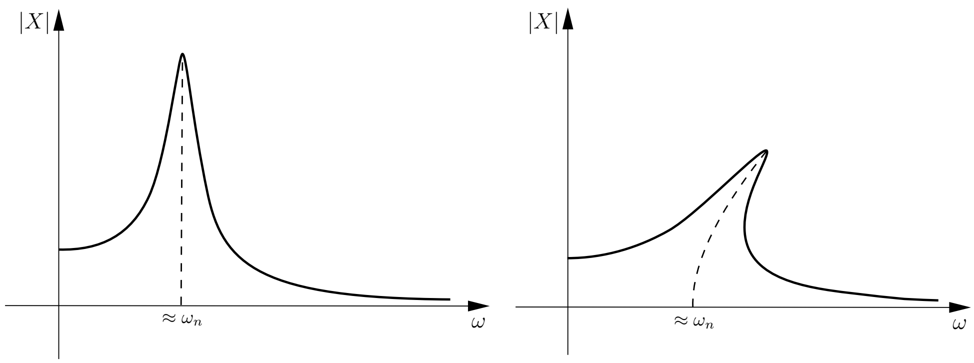

Figure 1: Comparison between a linear frequency response curve (left) and a nonlinear frequency response curve (right)

The equation of motion of an SDOF system with cubic stiffness (Duffing oscillator) is given by:

$$m\ddot{x} + c\dot{x} + kx + \beta x^3 = \frac{F}{2}e^{i\omega t} + \frac{F^*}{2}e^{-i\omega t}, \tag{15}$$

where x is the displacement, m the mass, c the damping coefficient and k the linear stiffness. β represents the nonlinear stiffness.

When it comes to SDOF linear systems with low damping, the peak occurs at approximately the undamped natural frequency $\omega_n = \sqrt{k/m}$. However, when nonlinear forces are present, such as βx^3, the undamped natural frequency changes as the oscillation amplitude increases. This modified undamped natural frequency is given by $\omega_n = \sqrt{k_{eq}/m}$ where the equivalent stiffness is $k_{eq} = k + \beta x^2$. If $\beta > 0$, indicating a positive nonlinear coefficient, the undamped natural frequency shifts towards the right as the equivalent stiffness increases. In this case, the oscillator exhibits the hardening phenomenon. Conversely, if $\beta < 0$, the system becomes less stiff as the amplitude increases, causing the resonance peak to tilt to the left. In this scenario, the oscillator shows the softening phenomenon.

4 THE ARC-LENGTH METHOD

The conventional algorithm for determining frequency response curves consists in solving the system equations in the frequency domain at a specific excitation frequency. Once the solution is computed, the excitation frequency is incremented, and the process is repeated until the entire frequency range of interest is covered. As seen in Figure 1, this method may prove unsuccessful when the oscillator exhibits the hardening or softening phenomena because, at some frequencies, at least three solution points are possible.

The arc-length method is a continuation algorithm that introduces an additional constraint equation to accurately determine curves with inflection points and instability zones. This constraint equation may take the form of a circle or ellipse for one-dimensional problems, sphere, cylinder or ellipsoid for two-dimensional problems, or hypersphere, hypercylinder or hyperellipsoid for problems with more than two dimensions.

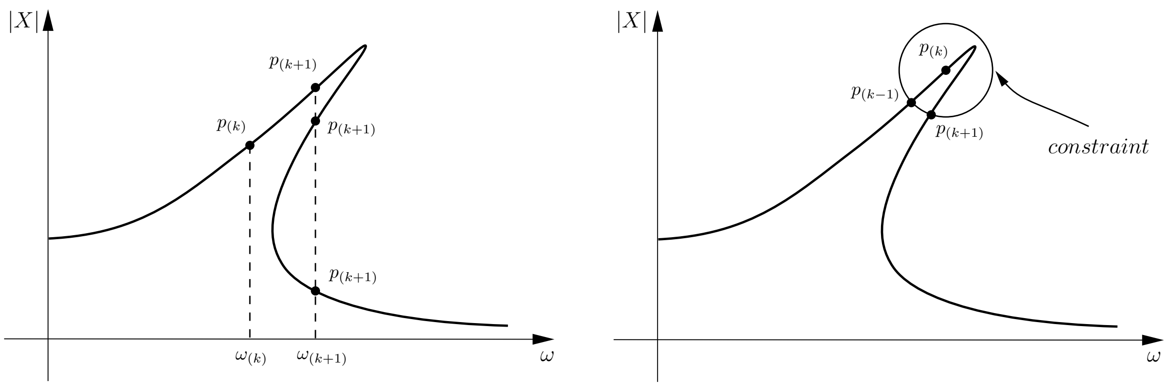

Figure 2: Comparison between a conventional algorythm (left) and the arc-length method to determine nonlinear frequency response curves

Figure 2 illustrates the difference between determining the frequency response curve simply by incrementing the excitation frequency versus applying the arc-length method. On the left, the converged solution point is denoted as $p_{(k)}$ at frequency $\omega_{(k)}$, and the next solution to be determined is at $\omega_{(k+1)}$. However, at this frequency, there exist three solution points. This problem can be overcome by adding the constraint equation of the arc-length method. With the constraint equation centered on the last converged solution point $p_{(k)}$, the next solution point $p_{(k+1)}$ can be correctly determined.

One drawback of the method is that the constraint equation intercepts the solution curve at least at two points. The arc-length method is an iterative algorithm divided into two phases: the first one, the predictor procedure, provides the initial approximation of the next solution point, determining the general direction of the next solution. If the solution direction is not chosen accurately, the algorithm may compute an already calculated solution point $p_{(k-1)}$. There are various criteria to determine the appropriate direction as seen in [13]. In this case, using the sign of the determinant of the matrix $\boldsymbol{K}_t$ proved effective for all cases considered in this paper, where $\boldsymbol{K}_t$ plays the same role as the tangent stiffness matrix in nonlinear static structural analysis. The second phase of the method is the corrector procedure, where the algorithm iterates the solution until convergence is achieved. When more than two points intercept the curve, it is necessary to decrease the arc-length radius to prevent the algorithm from failing.

5 NUMERICAL TESTS

In this section, four examples of nonlinear oscillators were analyzed. The first example is a Duffing oscillator with cubic stiffness only. The second example is a Helmholtz oscillator with quadratic stiffness. The final two examples exhibit both cubic and quadratic springs.

The high-order frequency response $H_{kl}^{[s]}$ is defined as the ratio of s-th harmonic of the complex displacement amplitude of the k-th degree-of-freedom (DOF), $X_k^{[s]}$, and the complex excitation amplitude apllied on the l-th DOF, F_l:

$$H_{kl}^{[s]} = \frac{X_k^{[s]}}{F_l}. \tag{16}$$

The time response of the s-th harmonic of the k-th DOF is $x_k^{[s]}$:

$$x_k^{[s]} = \frac{{X_k}^{[s]}}{2} e^{is\omega t} + \frac{{X_k}^{[-s]}}{2} e^{-is\omega t}. \tag{17}$$

5.1 The Duffing oscillator

The first numerical test consists in a single-degree-of-fredom (SDOF) Duffing oscillator. The equation of motion is given by Equation (15). Table 1 shows the physical parameters considered.

Table 1: Physical parameters of the Duffing oscillator

DOF	m (kg)	c (Ns/m)	k (N/m)	β (N/m^3)	F (N)
1	2	1	100	20	100

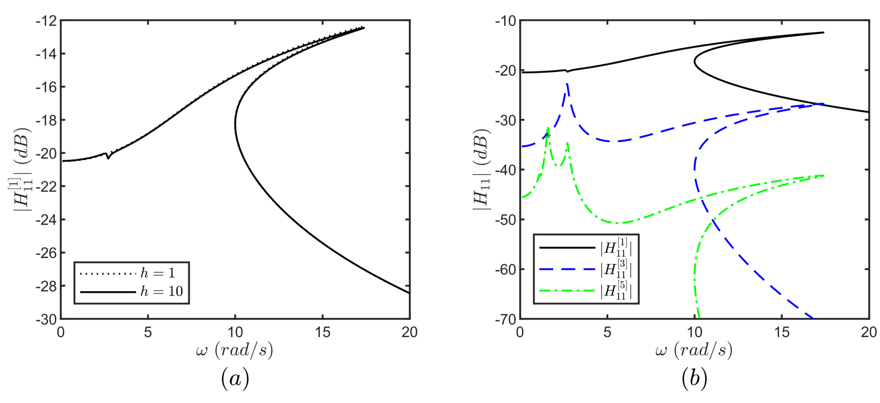

Figure 3: Frequency response curves for the Duffing oscillator

Figure $3a$ displays the first-order frequency response curve $H_{11}^{[1]}$ in two different scenarios: in the first one, only the fundamental harmonic is considered $(h = 1)$ while in the second, ten harmonics are considered in the system of equations $(h = 10)$. In this case, considering multiple harmonics has shown little difference compared to the first-order analysis. Figure $3b$ shows the high-order frequency response curves for $h = 10$, confirming Krack [10], that when it comes to the Duffing oscillator, the fundamental harmonic prevails over the high-order response. It is important to note that, in this case, the even frequency responses $H_{11}^{[2]}$, $H_{11}^{[4]}$, etc. were not significant, indicating that only the odd frequency responses are relevant.

5.2 The Helmholtz oscillator

The second numerical test consists in an SDOF Helmholtz oscillator. The equation of motion is given by Equation (18) with α as the quadratic stiffness:

$$m\ddot{x} + c\dot{x} + kx + \alpha x^2 = \frac{F}{2}e^{i\omega t} + \frac{F^*}{2}e^{-i\omega t}. \tag{18}$$

Table 2 shows the physical parameters considered.

Table 2: Physical parameters of the Helmholtz oscillator

DOF	m (kg)	c (Ns/m)	k (N/m)	α (N/m^2)	F (N)
1	1	0.3	100	1.5	100

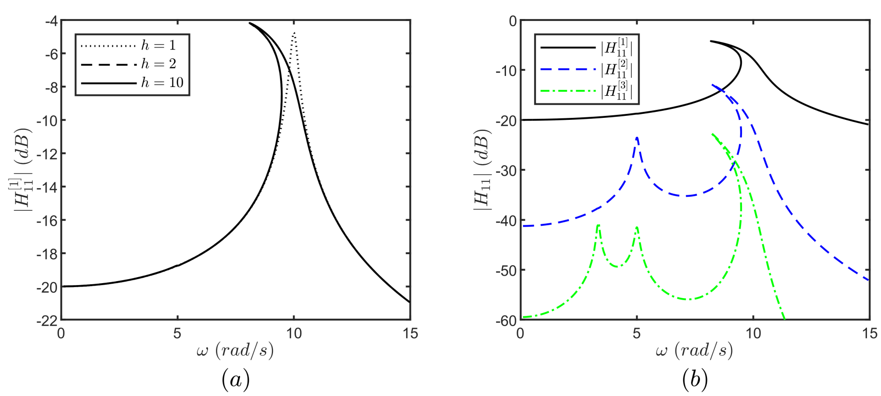

Figure 4: Frequency response curves for the Helmholtz oscillator

Figure $4a$ displays the first-order frequency response curve $H_{11}^{[1]}$ in three different scenarios: in the first one, only the fundamental harmonic is considered $(h = 1)$ without the static diplacement x_0. In the second, $h = 2$, two harmonics along with the static displacement, x_0, are considered, and finally, ten harmonics plus the static displacement are considered. In this case, considering multiple harmonics has shown great difference compared to the first-order analysis. The first-order frequency response is entirely different when only the fundamental harmonic is taken into account. Figure $4b$ illustrates the high-order frequency response curves for $h = 10$. It is crucial to note that not only does considering multiple harmonics drastically change the fundamental harmonic, but at certain frequencies, the high-order harmonics have an extremely impactful effect. Figure 5 displays the time domain response of the system at $\omega = 5.0\,rad/s$.

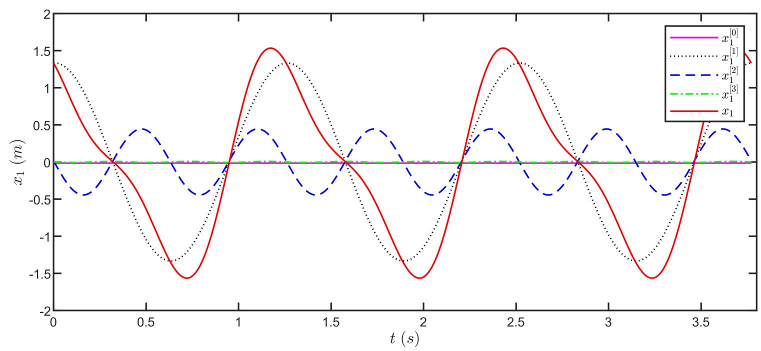

Figure 5: Time domain response at $\omega = 5.0\,rad/s$

5.3 The Duffing-Helmholtz oscillator

The third numerical test consists in an SDOF Duffing-Helmholtz oscillator with physical parameters shown in Table 3.

Table 3: Physical parameters of the SDOF Duffing-Helmholtz oscillator

DOF	m (kg)	c (Ns/m)	k (N/m)	α (N/m^2)	β (N/m^3)	F (N)
1	2	1	1 800	360	20	900

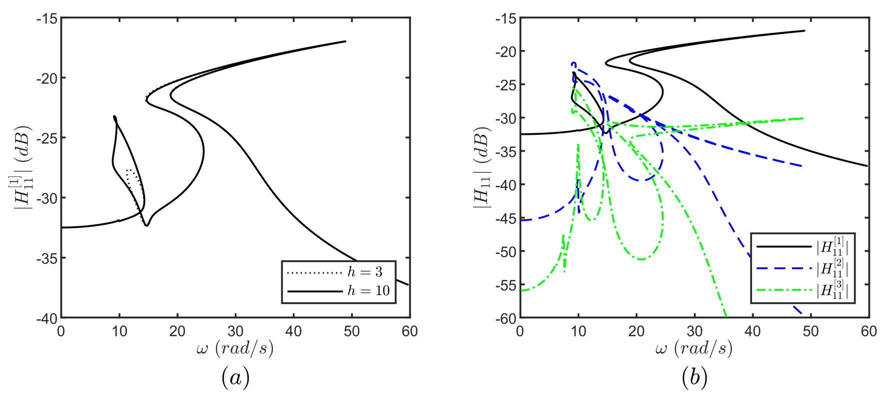

Figure 6: Frequency response curves for the SDOF Duffing-Helmholtz oscillator

Figure $6a$ displays the first-order frequency response curve $H_{11}^{[1]}$ in two different scenarios: in the first one, three harmonic are considered, in the second ten harmonics are considered. When considering three or fewer harmonics the algoryhtm has failed to correctly compute the frequency response curves. Only when six or more harmonics where considered the algorythm was capable of correctly compute the nonlinear forces. Figure $6b$ illustrates the high-order frequency response curves for $h = 10$. Figure 7 displays the time domain response of the system at $\omega = 9.3\, rad/s$.

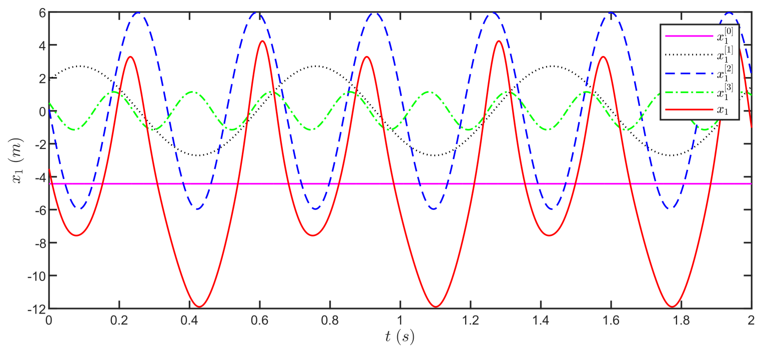

Figure 7: Time domain response at $\omega = 9.3\, rad/s$

The last numerical test consists in a 3DOF Duffing-Helmholtz oscillator with physical parameters shown in Table 4 and according to Figure 8.

Table 4: Physical parameters of the SDOF Duffing-Helmholtz oscillator

DOF	m (kg)	c (Ns/m)	k (N/m)	α (N/m^2)	β (N/m^3)	F (N)
1	2	0.40	4 000	200	4.20	1 520
2	1	0.30	3 000	150	5.46	0
3	1.8	0.07	2 800	175	6.30	0

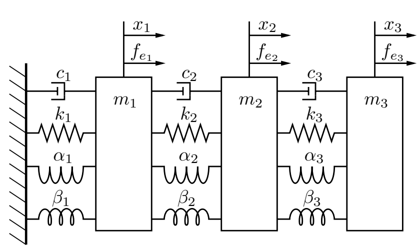

Figure 8: The 3DOF Duffing-Helmholtz oscillator

Similarly to the SDOF system, Figure $9a$ displays an inaccurate frequency response curve when only three harmonics were considered. The algorythm successfully determined the frequency response curves for six or more harmonics. Figure $9b$ illustrates the high-order frequency response curves for $h = 10$.

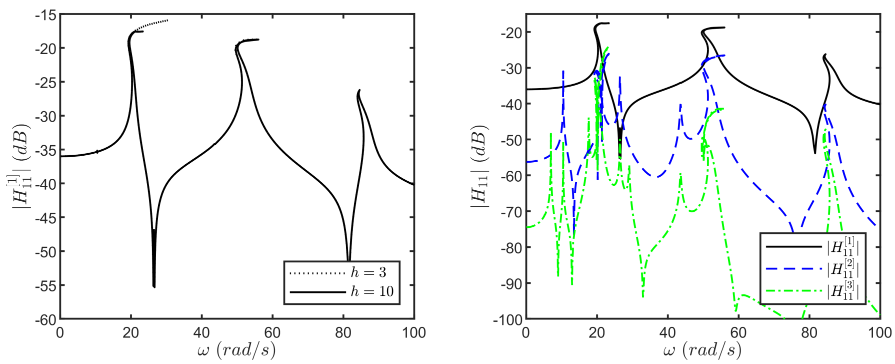

(a) (b)

Figure 9: Frequency response curves for the 3DOF Duffing-Helmholtz oscillator

6 CONCLUSIONS

This paper aimed to determine the high-order frequency response curves of nonlinear oscillators with cubic and/or quadratic springs. The arc-length method was applied and proved effective in overcoming instability zones and critical points. The high-order harmonic balance method accurately described responses at frequencies other than the excitation one.

The Duffin oscillator with only cubic stiffness proved to be well represented when only the first-order harmonic balance was implemented, showing insignificant results at higher frequencies. However, with the introduction of quadratic stiffness, not only did the determination of the first-frequency response rely on the higher-order harmonics, but at certain frequencies, the second and third-order harmonics had a meaningful impact on the system response.

7 ACKNOWLEDGMENTS

The authors thank Fundação de Amparo à Pesquisa do Estado de São Paulo (FAPESP), Grant Number 2017/15736-3, Conselho Nacional de Desenvolvimento Científico e Tecnológico (CNPq), Grant Numbers 307954/2022-6 and 130354/2021-0, for the financial support.

REFERENCES

[1] Riks, E. An incremental approach to the solution of snapping and buckling problems. *International Journal of Solids and Structures* (1979) **15**:529–551.

[2] Crisfield, M.A. A fast incremental/iterative solution procedure that handles “snap-through”. *Computers & Structures* (1981) **13**:55–62.

[3] Ferreira, J.V. and Serpa, A.L. Application of the arc-length method in nonlinear frequency response. *Journal of Sound and Vibration* (2005) **284**:133–149.

[4] Sowa, M. A Harmonic Balance Methodology for Circuits with Fractional and Nonlinear Elements. *Circuits, Systems, and Signal Processing* (2018) **37**:4695–4727.

[5] Hall, K.C., Ekici, K., Thomas, J.P. and Dowell, E.H. Harmonic balance methods applied to computational fluid dynamics problems. *International Journal of Computational Fluid Dynamics* (2013) **27**:52–67.

[6] Lewandowski, R. Non-linear, steady-state vibration of structures by harmonic balance/finite element method. *Computers & Structures* (1992) **44**:287–296.

[7] Tanrıkulu, Ö., Kuran, B., Özgüven, H. and İmregün, M. Forced Harmonic Response Analysis of Nonlinear Structures Using Describing Functions. *AIAA Journal* (1993) **31**:1313–1320.

[8] Kandil, A., Hamed, Y.S., Mohamed, S., Awrejcewicz, J. and Bednarek, M. Third-Order Superharmonic Resonance Analysis and Control in a Nonlinear Dynamical System. *Mathematics* (2022) **10**:1282–1298.

[9] Cochelin, B. and Vergez, C. A high order purely frequency-based harmonic balance formulation for continuation of periodic solutions. *Journal of Sound and Vibration* (2009) **324**:243–262.

[10] Krack, M. and Gross, J. *Harmonic Balance for Nonlinear Vibration Problems*. Springer International Publishing, Vol. I., (2019).

[11] Salas, H.A., Martinez, L.J. and Ocampo, D.L. Analytical and Approximate Trigonometric Solution to Duffing-Helmholtz Equation. *International Journal of Mathematics and Computer Science* (2021) **16**:1523–1531.

[12] Körner, T.W. and Tao, T. *Fourier Analysis*. Cambridge University Press, Vol. I., (2022).

[13] Neto, E.A. and Feng, Y.T. On the determination of the path direction for arc-length methods in the presence of bifurcations and 'snap-backs'. *Computer Methods in Applied Mechanics and Engineering* (1999) **179**:81–89.